Mechanism of PrP-amyloid formation in mice without transmissible spongiform encephalopathy

Published in final edited form as:
Brain Pathol. 2012 January ; 22(1): 58–66. doi:10.1111/j.1750-3639.2011.00508.x.

Mechanism of PrP-amyloid formation in mice without transmissible spongiform encephalopathy

Martin Jeffrey[1], **Gillian McGovern**[1], **Emily V. Chambers**[2], **Declan King**[2], **Lorenzo González**[1], **Jean C. Manson**[2], **Bernardino Ghetti**[3], **Pedro Piccardo**[2,3,4], and **Rona M. Barron**[2]

[1]Veterinary Laboratories Agency, Pentlands Science Park, Bush Loan Penicuik, Midlothian EH26 0PZ

[2]Neuropathogenesis Division, Roslin institute & R(D)SVS, University of Edinburgh, Roslin, Midlothian, EH25 9PS

[3]Indiana Alzheimer Disease Center and Division of Neuropathology, Indiana University School of Medicine, Indianapolis, IN 46202, USA

[4]Laboratory of Bacterial and TSE-agents, Food and Drug Administration, Rockville, MD20852 USA

Abstract

Gerstmann-Sträussler-Scheinker (GSS) P102L disease is a familial form of a transmissible spongiform encephalopathy (TSE) that can present with or without vacuolation of neuropil. Inefficient disease transmission into 101LL transgenic mice was previously observed from GSS P102L without vacuolation. However several aged, healthy mice had large plaques composed of abnormal prion protein (PrP^d). Here we perform the ultrastructural characterisation of such plaques and compare them with PrP^d aggregates found in TSE caused by an infectious mechanism. PrP^d plaques in 101LL mice varied in maturity with some being composed of deposits without visible amyloid fibrils. PrP^d was present on cell membranes in the vicinity of all types of plaques. In contrast to the unicentric plaques seen in infectious murine scrapie the plaques seen in the current model were multi-centric and were initiated by proto-fibrillar forms of PrP^d situated on oligodendroglia, astrocytes and neuritic cell membranes. We speculate that the initial conversion process leading to plaque formation begins with membrane-bound PrP^C but that subsequent fibrillisation does not require membrane attachment. We also observed that the membrane alterations consistently seen in murine scrapie and other infectious TSEs were not observed in 101LL mice with plaques suggesting differences in the pathogenesis of these conditions.

Keywords

amyloid plaques; prion protein; neurodegeneration; scrapie; Gerstmann-Sträussler-Scheinker

Introduction

Prion diseases or transmissible spongiform encephalopathies (TSEs) are a group of fatal neurodegenerative disorders that affect domestic farm animals, wild cervids, farmed mink and man. TSEs may be infectious under natural conditions or have an idiopathic or an iatrogenic cause, while in man they may also occur as a familial disorder (12). The pathological features of prion disease are usually cited as neuropil vacuolation, neuronal loss

Corresponding author M Jeffrey; m.jeffrey@vla.defra.gsi.gov.uk; tel 0131 445 6169; fax 0131 445 6166.

and gliosis. Prion diseases are characterised by the post translational conversion of a host encoded cellular isoform of prion protein (PrP^c) into pathologic isoforms (39) that may form amyloid plaques in affected subjects. Disease associated PrP may be detected by biochemical methods that involve a partial protease digestion step (PrP^{res}) while immunohistochemical methods reveal a variety of different membrane forms, aggregation states, and both protease resistant and protease sensitive forms of PrP (PrP^d). It is commonly thought that the pathologic isoforms of PrP may be infectious in the absence of nucleic acids (39). However, it is increasingly recognised that the correlation between PrP^d or PrP^{res} and infectivity is inexact (2, 3, 29, 38, 40). To accommodate discrepancies between PrP^d or PrP^{res} detection and infectivity, it has been proposed that sub-populations of abnormal PrP isofoms may exist that are pathogenic, protease sensitive and infectious while others are partially protease resistant and pathogenic but are not infectious (38, 43).

Gerstmann-Sträussler-Scheinker (GSS) disease is a familial prion disease associated with a variety of different mutations of the human prion protein gene *(PRNP*). Brains from human patients with some GSS mutations transmit a prion like disease to rodents or to primates (for review see (11)). One of the most studied GSS diseases is the proline to leucine mutation at codon 102 (P102L) (12). Two distinct phenotypes of GSS P102L disease have been described (36). In one phenotype PrP^{res} accumulates as 21 kDa and 8 kDa fragments, and is associated with vacuolation of the neuropil (35, 36) and transmissibility to wild type mice commonly used for laboratory bioassay (42) and PrP transgenic mouse lines (33, 38). The second disease phenotype is associated with only an 8 kDa PrP^{res} fragment and no neuropil vacuolation (36). When brain extracts from GSS P102L patients with 8kDa fragments and no vacuolation (PrP-8) are inoculated into wild type mice, no disease occurs. When such tissues are used to challenge a gene targeted transgenic mouse line which are homozygous for leucine at codon 101 (101LL; the mouse homologue of human codon 102) inefficient disease transmission is observed. However, several asymptomatic mice accumulate PrP amyloid plaques (101LL-8a mice), but do not replicate the TSE infectious agent. No neurological signs or vacuolation of the neuropil was observed in 101LL-8a mice on primary or subsequent sub-passage. However, recipient 101LL-8a mice also showed PrP amyloid accumulation on sub-passage (38). These amyloid plaques are composed of murine PrP^{res} suggesting that the human 8kDa P102L PrP^{res} can convert murine 101L PrP^c into murine PrP amyloid without creating infectivity or TSE. Thus 101LL-8a mice provide a model of mutant PrP interactions that result in amyloid plaque formation but no clinical disease or spongiform change.

That the conversion of host PrP^c to PrP^d may occur in the absence of infectivity is of some fundamental interest. Infectious TSEs of animals show a number of specific, mostly membrane related pathological changes (25). Cattle BSE, sheep scrapie, feline spongiform encephalopathy and different murine scrapie models all show membrane PrP^d accumulation associated with increased numbers of bizarre clathrin coated vesicles and clefts of dendrites, spiral membrane invaginations of axon terminals, membrane microfolding and increased lysosomes in brain (25). Some of these changes have been also been described in human TSEs but their co-localisation with PrP^d has not yet been confirmed. In this study we have sought to determine whether sub-cellular features of pathological changes that uniquely occur in infectious TSEs are also present in 101LL-8a mice and to study the nature of the conversion process of 101LL PrP^c into amyloid. We show that unlike PrP^d accumulations found in most naturally infectious forms of TSEs, 101LL-8a mice form amyloid fibrils without such membrane pathology. We further show that fibrils are generated from putative protofilaments by recruitment of PrP^c molecules attached to cell membranes.

Materials and methods

The generation of 101LL mice (33) and the results after inoculation of PrP-8 has previously been described (38). The human brain tissue used in these original studies was obtained with full consent of the patient's family for use in research. All mouse experiments were reviewed and approved by the Local Ethical Review Committee and performed under license from the United Kingdom Home Office in accordance with the United Kingdom Animals (Scientific Procedures) Act 1986.

Brains from 14 101LL-8a mice at more that 400 days after intracerebral challenge with brain homogenate from mice previously challenged with 8kDa GSS P102L(101LL-8a mice) were embedded in paraffin wax, cut and labeled with antibodies raised to mouse PrP by methods in routine use in our laboratory (14). The R18 antibody was raised against amino-acid sequence (aa) 142-155; R20 to aa 218-232; R24 to aa 23-37 and R30 to aa 89-103 as previously reported (6). The number and location of plaques in five coronal whole brain or hemi-brain slices, two of which contained representation of the corpus callosum, were recorded in each mouse.

An additional four 101LL mice inoculated with brain homogenate from 101LL-8a mice were killed at 626-638 days of age post challenge together with three unchallenged age matched controls. These mice were perfused with 4% paraformaldehyde and 0.1% glutaraldehyde for study by electron microscopy and their brains were serially coronally sectioned at 1mm intervals. Alternate serial 1mm brain slices were then embedded in paraffin wax, sectioned and immuno-labeled for PrP^{d} to confirm the presence and distribution of plaques by light microscopy. Other brain slices were further sectioned to $1mm^3$ samples. These tissue blocks were post-fixed in osmium tetroxide, dehydrated and embedded in epon resin for electron microscopy. Between 21 and 30 one mm^3 cube blocks of brain tissue (cerebellum, thalamus and hippocampus) were taken from each mouse.

101LL mice develop disease when challenged with brains of GSS P102L patients that demonstrate vacuolation and accumulation of both 21kDa and 8kDa PrP^{res} fragments (38). However such mice do not reliably develop plaques and plaques could not be found in samples prepared from three such mice prepared for electron microscopy. 87V scrapie is an infectious murine scrapie strain which produces accumulation of numerous PrP^{d} plaques in VM mice (19). Only higher molecular weight fragments of PrP^{res} and not the 8kDa PrP^{res} fragment can be demonstrated from brains of mice with 87V scrapie (19). Accordingly, 87V murine scrapie and unchallenged transgenic mice were used as controls.

Our previous experience indicates that not all antibodies able to detect PrP^{d} in wax embedded tissues can reveal PrP^{d} in tissues embedded in plastic (18).To identify antibodies for use in immunogold electron microscopy a range of antibodies were tested in wax and plastic embedded tissues. The following anti-PrP monoclonal antibodies were selected for testing: i) BG4 and Saf32, which were raised against bovine recombinant PrP aa 23-85 or sheep aa 62-90 respectively and both recognize sequences within the octapeptide repeat region that are conserved in the mouse; ii) Saf 84, Sha 31 and 2G11 raised against different PrP aa 145-182 of the sheep sequence; iii) polyclonal rabbit antibodies R486 raised against bovine PrP aa 217-231 and 1A8 raised against a murine scrapie-associated fibril preparation.

Each of the above antibodies was able to recognize PrP^{d} in wax embedded tissues of 101LL-8a mice. PrP^{d} plaques in plastic embedded tissues were only revealed by 1A8, R486 and Saf 84 antibodies. Therefore, the other antibodies listed above were not taken though to immunogold electron microscopy and will not be discussed further.

Sections obtained from wax embedded tissues were also labeled by immunohistochemistry for glial fibrillary acidic protein (Dako Uk ltd). Additional sections were stained by haematoxylin and eosin, by periodic acid Schiff reaction or by Congo red methods.

Electron microscopy procedure

Resin embedded sections were cut at 1μm and stained with toluidine blue or labeled with 1A8, R486 or Saf 84. Tissues from mice infected with 87V scrapie were available as positive controls. As described previously (34) the avidin-biotin complex immunohistochemical staining method was applied to the etched and pre-treated sections.

Uni-centric plaques and plaques with multi-centric cores were identified in several tissue blocks taken from each of three 101LL-8a mice. Sections from five blocks, each containing from one to five plaques, were then serially sectioned at 60nm and stained using uranyl acetate and lead citrate. Sections were then immuno-labelled for PrP^d using 1A8, Saf84 or R486 antibodies by immunogold methods as previously described (34).

Using these post-embedding immunogold methods, no immuno-labelling is found in control mouse brains (not shown). Thus PrP^c is not detected in normal mouse brains (not shown) by the post-embedding methods employed here and all immuno-labelling found in disease affected brains is interpreted as PrP^d.

Results

Light microscopy

Where serial sections of brains embedded in paraffin wax were examined, 10 of 14 101LL-8a mice showed the presence of PrP^d plaques. In all but two mice, plaques were located in or adjacent to the corpus callosum. The remaining plaques found in two mice were within the internal capsule, adjacent to the pia of the ventral hippocampus or dorsal thalamus and within the s*tratum lacunosum* of the hippocampus. Only hemi-brain slices were available from most mice but a bilateral distribution of plaques was confirmed in two mice where whole brains were available. Plaques in the hemisphere contra-lateral to the injection hemisphere were also located in the corpus callosum. The pattern of labelling of plaques was the same for each of the antibodies used in this study. While a proportion of plaques showed uniform labelling, most showed a weaker immunoreactivity in the core of the plaques and a stronger labelling intensity in the plaque periphery (Fig 1). This pattern was the same for C- (R18, R20, R30, R486, 1A8, Saf 84, Sha 31 2G11) and N-terminal (R24; BG4; Saf 32) antibodies, and for tissues fixed in formaldehyde and embedded in paraffin wax or fixed in mixed aldehydes and embedded in paraffin wax or in plastic. In contrast with the plaques in 101LL-8a mice, plaques from 87V infected mice were consistently and uniformly labelled with all antibodies tested in both core and periphery (Fig 1).

A range of plaque morphology was seen in 101LL-8a mice. Some large uni-centric plaques were round or ovoidal while other multi-centric plaques consisted of a large dense core surrounded by smaller irregular areas of labelling (Fig 1a). Multifocal groups of plaques and localised peri-cellular PrP^d labelling patterns were also seen (Fig 1b). When the numbers of plaques were compared in HE or toluidine blue labelled sections and in serial immuno-labelled sections, many fewer plaques were detected by tinctorial staining methods. More plaques were also seen on immuno-labelled sections when compared to sections stained by the periodic-acid Schiff reaction or by Congo red, suggesting that not all plaques were composed of mature amyloid arranged into bundles.

87V plaques had the classical stellate appearance and were not multi-centric.

Electron microscopy 101LL-8a: uranyl acetate-lead citrate staining

Some plaques were entirely contained within the corpus callosum but many were at the interface of the ventral border of the corpus callosum and the hippocampus and often spilled over to involve the *stratum oriens*. Within the corpus callosum plaques were situated between planes of white matter where one group of myelinated processes was running at an angle different from an adjacent bundle. Often the plaques were located around or near blood vessels. Plaques entirely located within white matter of the corpus callosum were surrounded by reactive astrocytes or oligodendroglia. Microglia were infrequent in white matter plaques but were more prominent around plaques that extended into the *stratum oriens* of the hippocampal grey matter.

Multi-centric plaques were generally composed of a dense core (Fig 2a) and several peripherally located, similarly sized, satellite sub-units (Fig 2c). The core of large plaques consisted almost exclusively of densely packed and randomly orientated amyloid fibrils (Fig 2a). Serial sectioning through multi-centric plaques suggested that each satellite sub-unit derived from a separate core or seed. Thus satellite plaques surrounding large dense parent plaques appear to be initiated from centrifugally dispersed seeds rather than emanating by continuous growth from the parent core. A spectrum of maturity of multi-centric plaques could be inferred from their structure. While older, more mature multi-centric plaques are as described above, other less mature multi-centric plaques consisted of sub-units possessing few amyloid fibrils surrounded by reactive glial processes (Fig 2d,e) suggesting a continuous and ongoing process of seeding and growth.

The periphery of large parent and satellite plaques showed smaller groups of amyloid fibrils inserted between different cellular processes (Fig 2b) and surrounded by reactive microglia, astrocytes and large dystrophic neurites (Fig 2f). Dystrophic neurites, which are characterised by the accumulation of excess organelles including lysosomes and mitochondria (31), affected both large myelinated fibres and smaller unmyelinated neurites. Individual dystrophic processes and other degenerative white matter features such as axons undergoing Wallerian-type degeneration could be found at some considerable distances (at least 0.5 mm) from a plaque.

Electron microscopy 101LL-8a: immunogold labelling

The cores of plaques in 101LL-8a mice, which consisted of densely packed randomly orientated fibrils, (that were unstained or lightly stained in 1μm thick sections), were labelled for PrP^d by immunogold methods (Fig 3a). Those cores were labelled successfully by all three antibodies used 1A8, R486, and by Saf84. Because fibrils in the centre of amyloid plaques that were unlabelled by antibodies in 1μm plastic embedded sections were labelled when the same antibody was used on serial immunogold labelled sections cut at 60-80nm thickness, it would appear that the absence of labelling was due to technical issues, probably related to the highly compact nature of the packing of the amyloid fibrils in these plaques.

Satellite plaques (Fig 3b) at the periphery of large plaques, consisting of smaller groups of extracellular amyloid fibrils and smaller multi-centric plaques, also showed labelling for PrP^d with each of the antibodies used. However, PrP^d labelling was not confined to amyloid fibrils. At the extreme periphery of uni-centric plaques and larger multi-centric plaques, PrP^d labelling was found on the cell membranes of processes and on cell bodies in the absence of visible fibrillar amyloid (Fig 3c). PrP^d plasma-lemmal labelling surrounding plaques located in corpus callosum white matter was found on oligodendroglia (Fig 3c) and astrocytes (Fig 3d). Where plaques extended to involve grey matter, PrP^d membrane labelling was also seen on dendrites and probably also on axonal membranes.

Some plaques visible in immuno-labelled 1μm thick sections examined by light microscopy could not be reliably located by uranyl acetate /lead citrate staining but could be detected following immunogold labelling for PrP^d in serial sections. PrP^d labelling of such nascent plaques consisted of localised areas of membrane and extracellular PrP^d signal (Fig 3e). In uranyl acetate/lead citrate stained sections these plaques could only be found by determining the location of the plaque in immunogold labelled sections, and then finding the exact same location in the uranyl acetate/lead citrate stained sections. These nascent plaques showed none of the pathological changes associated with the more mature plaques: there was no evidence of amyloid fibrils, gliosis, or neuronal dystrophia and only mild irregularity of process contours could be identified.

Membrane-associated PrP^d in the infectious forms of animal TSEs is associated with several specific membrane changes (vide infra and (25)). These changes were not found in the 101LL-8a mice. Also present in naturally occurring TSEs and experimental models of scrapie is lysosomal PrP^d accumulation in neuronal perikarya and in astrocytes and microglia (25). The latter are often particularly abundant around plaques. In the 101LL-8a mouse, PrP^d was absent from lysosomes of astrocytes and microglia.

Dystrophic neurites were not found in the centre of plaques, rather they were predominantly located at the plaque periphery within areas of neuropil containing small numbers of amyloid fibrils in the extracellular spaces. Although strong immunogold labelling was obtained on these amyloid fibrils and on some adjacent cell membranes, PrP^d labelling was not specifically detected on cell membranes of dystrophic neurites, nor was PrP^d labelling found on the cell membranes of oligodendrocytes or axons associated with other degenerative white matter lesions.

Electron microscopy: 87V scrapie

The morphology and inferred formation of plaques in 87V scrapie was in agreement with previous descriptions (19,20). Briefly, plaques in 87V scrapie occurred mainly in grey matter where they appeared to be initiated by accumulation of PrP^d at short segments of dendrite plasma-membranes and then locally released to form small numbers of visible short amyloid fibrils lying between processes. These short amyloid fibrils elicited marked astrocytic and microglial responses. With increasing plaque maturity, individual fibrils were orientated into bundles and plaques took the classic stellate appearance by a centrifugal growth of these amyloid bundles radiating between cell processes within grey matter neuropil. Diffuse plaques with fewer fibrils and lacking a stellate arrangement were also found adjacent to the glial limitans of the sub-pial neuropil and within the thalamus. White matter plaques were occasionally found in the corpus callosum. Plaques were surrounded by dystrophic neurites, reactive astrocytes and microglia.

As previously reported, strong PrP^d labelling was observed on amyloid fibrils (Fig 4a) (19, 20). PrP^d labelling was also found on dendrite membranes of immature plaques and where only sparse, or no fibrils were seen at the plaque periphery (Fig 4b). Also present at these locations were microglia and astrocytes with immuno-labelling for PrP^d within lysosomes (Fig 4c). At the extreme periphery of the plaque, membrane changes pathognomonic of infectious TSEs were also seen (25) (Fig 4d-g). These changes consisted of membrane protrusions or micro-folding (Fig 4d,e), spiral membrane inclusions in axon terminals (Fig 4f), abnormal dendritic membrane invaginations and excess coated pits (Fig 4g). For a more complete description of the nature and morphologic variation of these TSE-specific membrane changes see (25). In addition, other prion specific changes such as so called tubulovesicular bodies and non-prion specific changes such as axon terminal degeneration and vacuolation were also present within neuropil in the vicinity of plaques (not shown).

Discussion

In this study we have shown that the plaques found in 101LL-8a mice consisted not only of mature plaques composed of densely packed amyloid fibrils, but also of focal plaque-like PrP^d accumulations that lacked any discernable amyloid fibrils by electron microscopy. PrP^d surrounding mature plaques could be found in the absence of fibrillar amyloid apparently still attached to the plasma-membranes of cells and processes. Similarly, newly forming plaques appeared to be generated by similar interactions also at the plasma-membrane of PrP^c expressing cells. These observations indicate that new plaques continue to be seeded and mature plaques continue to grow even after more than 600 days after challenge. Plaques appear to be initiated by a process in which sub-fibrillar PrP^d aggregates (proto-filaments or oligomers) spread through the extracellular space to recruit and convert new PrP^c molecules that are still attached to membranes.

In vitro studies of the PrP^c-PrP^{res} conversion reaction have shown that microsomal PrP^c attached to detergent resistant membranes of neuroblastoma cells was not converted by simple incubation with microsomes containing membrane attached PrP^{res} (1). Conversion of PrP^c was only achieved when PrP^c and PrP^{res} were placed in the same membrane plane by fusing microsomal PrP^c with other membranes containing PrP^{res}. These data suggested that seed PrP^{res} required to be inserted into microsomal membranes prior to the induction of new PrP^{res} molecules (1). Our observations agree with these in *vitro* data and suggest that *in situ*, the PrP^c substrate for conversion is retained at the plasma-membrane where it is converted by exogenously derived oligomers of PrP^d. The electron microscopy does not indicate whether exogenous PrP^d first inserts into the membrane prior to seeded conversion of new PrP^c molecules but membrane insertion of soluble, globular, pre-fibrillar amyloid oligomers appear to be an intrinsic property of different amyloid proteins (27).

While *in vitro* and *in vivo* data agree that seeded conversion of PrP^c to PrP^d or PrP^{res} appears to be initiated by contact between PrP^d or PrP aggregates and membrane localised PrP^c, this is unlikely to be the mechanism which supports plaque growth. Studies of microsomal PrP^c show that conversion to PrP^{res} may also occur when PrP^c is released from membranes by cleavage of the glycophosphatidylinositol (GPI) anchor that attaches it to the outer cell membrane (1). However, other *in vitro* approaches have suggested that the release of PrP^c from membranes of neuroblastoma cells may actually inhibit the formation of PrP^{res} (5). Large, and numerous plaques may be found in scrapie infected mice engineered to produce PrP^c molecules lacking the GPI anchor (7). As PrP^c is not retained at cell membranes in this model it cannot be converted there and plaques formed in these anchorless mice are formed by soluble forms of PrP^c released to the extracellular space that subsequently aggregate in and around blood vessels. In the 101LL-8a mouse we can also infer continued growth of large, immobile, plaques at their periphery where there are few cellular processes with attached membrane PrP^c. It is likely therefore that some PrP^c molecules or newly formed oligomers of PrP^d may be released from membranes to continue the growth of 101LL-8a plaques by adding onto the ends of immobilised amyloid fibrils within the extracellular space.

The plaques which form in the infectious TSEs such as murine 87V scrapie are invariably uni-centric and appear to form initially at the plasma membranes of dendrites (19). Although multiple plaques may form along the length of a dendrite, scrapie plaques, unlike GSS plaques, are not conspicuously multi-centric. Multi-centric plaques in 101LL-8a mice mostly consisted of a single large core with several smaller satellite sub-units surrounding them. The sub-unit satellites of multi-centric plaques are probably formed by the spread of oligomers fragmenting from the main plaque and spreading through the interstitial space until they are stabilised *in situ* following new conversion reactions with PrP^c molecules on

plasma-membranes of adjacent cells. The present observations suggest that the conversion of PrP^c to amyloid possesses several steps that are common to both 87V scrapie and 101LL-8a. These steps are the conversion of PrP^c to PrP^d at the cell membranes, the release of converted PrP^d into the extracellular space and the subsequent ordering of PrP^d aggregates into large bundles of amyloid fibrils. However, both the gross arrangement of amyloid plaques and the nature of the membrane changes present in 87V scrapie point to the existence of other distinguishing disease processes.

In scrapie of sheep, BSE of cattle and feline spongiform encephalopathy as well as in experimental scrapie models of mice, there are a number of distinctive membrane changes that are both directly linked to PrP^d and appear to be unique to TSE disease (10, 23, 24, 25). These changes, which include the abnormal membrane protrusions or microfolds, and spiral membrane invaginations of axon terminals illustrated in 87V scrapie were absent from 101LL-8a mice. The PG14 mouse is another transgenic line which mimics a GSS insertional mutation of PrP and it also lacks these membrane changes (17). The PG14 mouse is also not infectious to wild type mice or to other mice over-expressing the same mutation (9). Thus TSE specific membrane pathology is found only in infectious TSEs.

Dystrophic axons were conspicuous around plaques of 101LL-8a mice. Dystrophic processes are also prominent around the cerebrovascular plaques of the scrapie infected anchorless mouse (7); the stellate plaques formed in 87V scrapie (present observations and (19)) as well as several other human prion diseases and murine models (26, 30). Although rare dystrophic neurites are also found in normal brain tissue, they are increased in several chronic non-prion human neurodegenerative diseases (30) and are a particular feature associated with Alzheimer's disease plaques(31). Thus dystrophic neurites are consistently present both in prion and in non-prion disorders where abundant amyloid is formed irrespective of the protein composition of the amyloid. While the mice in this study did not get sick the scrapie infected GPI anchorless mice do so, but with clinical signs and disease progression not typical of the RML scrapie strain used to infect them (4, 8). We suggest that amyloid may result in degenerative disease processes that may result in neurological deficits in their own right. Dystrophic neurites and Wallerian-type axonal degeneration are evidence of this amyloid related damage. However, the 101LL-8a mice did not show clinical disease probably because of the relative infrequency of plaque formation. As many naturally occurring infectious TSEs diseases do not form plaques it is unlikely that neurological deficits in the infectious prion diseases are significantly related to such changes.

The role of glial cells in the genesis and maintenance of plaques in Alzheimer's disease has been questioned over many years. According to some, microglia are instrumental in assembling fibrils for the formation of both scrapie and Aß amyloid plaques (45). In the 101LL-8a mouse both activated microglia and reactive astrocytes were prominent at the periphery of plaques where amyloid bundles could be seen engulfed by highly indented microglial membranes. However, activated microglia are absent where PrP^d was confined solely to membranes and also from some plaques that were contained entirely within white matter of the corpus callosum. These observations suggest those microglial cells are not essential for PrP^c–PrP^d conversion or for arranging PrP^d into highly ordered fibrils. The generation of Aß plaques has been studied in APP transgenic mice crossed with other transgenic mice expressing a chemically activated microglial suicide gene (15). In this Alzheimer's disease model microglial cells were ablated without effect on numbers of plaques over the course of disease suggesting that microglia are neither necessary to initiate nor to maintain Aß plaques. Thus microglia do not appear to be necessary for generation of plaques of 101LL-8a mice nor murine Aß plaques. Similarly, in the APP mouse model the numbers of dystrophic neurites were not altered in the presence of activated microglial cells suggesting the cytokines released by glia do not play a significant part in their origins (15).

Although the highest expression of PrP^c appears to be on neurons (32), the source of PrP^c for conversion into new amyloid plaques or to continue growth of existing plaques in 101LL-8a mice may involve several cell types. Plaques that are entirely contained within the corpus callosum have contact only with astrocytes, oligodendroglia, and cells surrounding blood vessels. Immuno-labelling for PrP^d at extreme plaque peripheries showed membrane associated PrP^d on the plasmalemmas of oligodendroglia and astrocytes. Where plaques extended to the stratum *oriens* of the hippocampus, plasmalemmal labelling was found on neurites, including dendrites and possibly also axons. Thus PrP^c substrate for conversion to PrP^d could be provided by oligodendroglia, astrocytes or neurites.

Previous studies of the nature of amyloid plaques in GSS patients had shown that the amyloid is composed only of protein derived from the mutant allele (41). Other studies have suggested that the non-mutant allele may also be involved and may influence disease phenotype, including the pathological phenotype of some GSS P102L patients (44). However, it is not clear whether this latter study is relevant to the current study as analysis of plaques generating 8kDa fragments is not mentioned. In other immunohistochemical studies of the plaques of GSS patients, including GSS P102L, it was found that PrP antibodies recognising N terminal epitopes failed to label plaque cores (13, 16, 28, 37). This has led some authors to suggest that amyloid plaques were initially composed of full length PrP^{res} that became progressively truncated. In contrast, both the core and the periphery of plaques formed in infectious TSEs are labelled with antibodies to both N and C terminal amino acids (21, 22). In the present study none of three PrP antibodies used at the light microscopy level labelled the cores of 101LL-8a plaques but the same antibodies labelled core fibrils when immunogold electron microscopy was performed. When compared with 87V plaques individual fibrils of 101LL-8a plaques are more densely packed suggesting that the absence of core staining of 101LL-8a plaques at light microscopy may be due to poor antibody penetration of these latter plaques. It would therefore appear likely that fibrils in 101LL-8a plaques are formed from full length PrP protein as they are in 87V scrapie.

In this study we have shown that small PrP^d seeds can drive *in situ* conversion of PrP^c located on cell membranes. Such conversion is not restricted by cell type but the further growth of amyloid fibrils appears to require release of pre-formed PrP^d into the extracellular space. PrP^c conversion and growth of amyloid fibrils can occur without generating TSE infectivity, whereas the membrane changes that are found in truly infectious TSEs are not present in association with these amyloid structures.

Acknowledgments

Thanks to Byron Caughey, Rocky Mountain Laboratories, MT, USA for antibodies R18, R20, R24 and R30. These studies were partly funded by the Biotechnology and Biological Sciences Research Council (BBSRC), Defra grant Se1790 and NIH-NIAID Agreement No.Y1-AI-4893-02 and FDA Agreement No. 224-05-*1307*. The findings and conclusions in this article have not been formally disseminated by the Food and Drug Administration and should not be construed to represent any Agency determination or policy. Prof. Ghetti is supported by grant PHS P30 AG 10133.

Reference List

[1]. Baron GS, Wehrly K, Dorward DW, Chesebro B, Caughey B. Conversion of raft associated prion protein to the protease-resistant state requires insertion of PrP-res (PrPSc) into contiguous membranes. *Embo* J. 2002; 21:1031–1040. [PubMed: 11867531]

[2]. Barron RM, Campbell SL, King D, Bellon A, Chapman KE, Williamson RA, Manson JC. High titers of transmissible spongiform encephalopathy infectivity associated with extremely low levels of PrPSc in vivo. J Biol Chem. 2007; 282:35878–35886. [PubMed: 17923484]

[3]. Barron RM, Thomson V, King D, Shaw J, Melton DW, Manson JC. Transmission of murine scrapie to P101L transgenic mice. J Gen Virol. 84:3165–3172. [PubMed: 14573822]

[4]. Caughey B, Baron GS, Chesebro B, Jeffrey M. Getting a grip on prions: oligomers, amyloids, and pathological membrane interactions. Annu Rev Biochem. 2009; 78:177–204. [PubMed: 19231987]

[5]. Caughey B, Raymond GJ. The scrapie-associated form of PrP is made from a cell surface precursor that is both protease- and phospholipase-sensitive. J Biol Chem. 1991; 266:18217–18223. [PubMed: 1680859]

[6]. Caughey B, Raymond GJ, Ernst D, Race RE. N-Terminal truncation of the scrapie-associated form of PrP by lysosomal protease(s): Implications regarding the site of conversion of PrP to the protease-resistant state. J Virol. 1991; 65:6597–6603. [PubMed: 1682507]

[7]. Chesebro B, Race B, Meade-White K, LaCasse R, Striebel J, Klingeborn M, Race R, McGovern G, Dorward D, Jeffrey M. Fatal transmissible amyloid encephalopathy: a new type of prion disease associated with lack of prion protein membrane anchoring. Plos Pathogens. 2010:e1000800. [PubMed: 20221436]

[8]. Chesebro B, Trifilo M, Race R, Meade-White K, Teng C, LaCasse R, Raymond L, Favara C, Baron G, Priola S, Caughey B, Masliah E, Oldstone M. Anchorless prion protein results in infectious amyloid disease without clinical scrapie. Science. 2005; 308:1435–1439. [PubMed: 15933194]

[9]. Chiesa R, Piccardo P, Quaglio E, Drisaldi B, SiHoe SL, Takao M, Ghetti B, Harris DA. Molecular distinction between pathogenic and infectious properties of the prion protein. J Virol. 2003; 77:7611–7622. [PubMed: 12805461]

[10]. Ersdal C, Goodsir CM, Simmons MM, McGovern G, Jeffrey M. Abnormal prion protein is associated with changes of plasma membranes and endocytosis in bovine spongiform encephalopathy (BSE)-affected cattle brains. Neuropathol Appl Neurobiol. 2009; 35:259–271. [PubMed: 19473293]

[11]. Gambetti, P.; Petersen, RB.; Parchi, P.; Chen, SG.; Capellari, S.; Goldfarb, L.; Gabizon, R.; Montagna, P.; Lugaresi, E.; Piccardo, P.; Ghetti, B. Inherited prion diseases. In: Prusiner, SB., editor. Prion Biology and Diseases. Cold Spring Harbor Laboratory Press; 1999. p. 509-583.10 Skyline Drive/Plainview/NY 11803-2500/USA

[12]. Ghetti B, Piccardo P, Frangione B, Bugiani O, Giaccone G, Young K, Prelli F, Farlow MR, Dlouhy SR, Tagliavini F. Prion protein amyloidosis. Brain Pathol. 1996; 6:127–145. [PubMed: 8737929]

[13]. Giaccone G, Verg L, Buggiani O, Frangione B, Servan D, Prusiner SB, Farlow MR, Gjetto B, TagliaviniI F. Prion protein preamyloid and amyloid deposits in Gerstmann-Straussler-Scheinker disease, Indiana kindred. Proc Natl Acad Sci USA. 1992; 89:9349–9353. [PubMed: 1357663]

[14]. González L, Martin S, BegaraMcGorum I, Hunter N, Houston F, Simmons M, Jeffrey M. Effects of agent strain and host genotype on PrP accumulation in the brain of sheep naturally and experimentally affected with scrapie. J Comp Pathol. 2002; 126:17–29. [PubMed: 11814318]

[15]. Grathwohl SA, Kalin RE, Bolmont T, Prokop S, Winkelmann G, Kaeser SA, Odenthal J, Radde R, Eldh T, Gandy S, Aguzzi A, Staufenbiel M, Mathews PM, Wolburg H, Heppner FL, Jucker M. Formation and maintenance of Alzheimer's disease beta-amyloid plaques in the absence of microglia. Nat Neurosci. 2009; 12:1361–1363. [PubMed: 19838177]

[16]. Hashimoto K, Mannen T, Nukina N. Immunohistochemical study of Kuru plaques using antibodies against synthetic prion protein peptides. Acta Neuropathol. 1992; 83:613–617. [PubMed: 1353279]

[17]. Jeffrey M, Goodsir C, McGovern G, Barmada SJ, Medrano AZ, Harris DA. Prion protein with an insertional mutation accumulates on axonal and dendritic plasmalemma and is associated with distinctive ultrastructural changes. Am J Pathol. 2009; 175:1208–1217. [PubMed: 19700753]

[18]. Jeffrey, M.; Goodsir, CM. Immunohistochemistry of resinated tissues for light and electron microscopy. In: Baker, HF.; Ridley, RM., editors. Prion Diseases. Humana Press; 1996. p. 301-312.

[19]. Jeffrey M, Goodsir CM, Bruce ME, McBride PA, Farquhar C. Morphogenesis of amyloid plaques in 87V murine scrapie. Neuropathol Appl Neurobiol. 1994; 20:535–542. [PubMed: 7898615]

[20]. Jeffrey M, Goodsir CM, Bruce ME, McBride PA, Scott JR, Halliday WG. Correlative light and electron microscopy studies of PrP localization in 87V scrapie. Brain Res. 1994; 656:329–343. [PubMed: 7820594]

[21]. Jeffrey M, Goodsir CM, Fowler N, Hope J, Bruce ME, McBride PA. Ultrastructural immuno-localization of synthetic prion protein peptide pntibodies in 87V Murine Scrapie. Neurodegeneration. 1996; 5:101–109. [PubMed: 8731389]

[22]. Jeffrey M, Goodsir CM, Holliman A, Higgins RJ, Bruce ME, McBride PA, Fraser JR. Determination of the frequency and distribution of vascular and parenchymal amyloid with polyclonal and N terminal specific PrP antibodies in scrapie -affected sheep and mice. Vet Rec. 1998; 142:534–537. [PubMed: 9637378]

[23]. Jeffrey M, Goodsir CM, Race RE, Chesebro B. Scrapie-specific neuronal lesions are independent of neuronal PrP expression. Ann Neurol. 2004; 55:781–792. [PubMed: 15174012]

[24]. Jeffrey M, McGovern G, Goodsir CM, Gonzalez L. Strain-associated variations in abnormal PrP trafficking of sheep scrapie. Brain Pathol. 2009; 19:1–11. [PubMed: 18400047]

[25]. Jeffrey M, McGovern G, Siso S, Gonzalez L. Cellular and sub-cellular pathology of animal prion diseases: relationship between morphological changes, accumulation of abnormal prion protein and clinical disease. Acta Neuropathol. 2011; 121:113–134. [PubMed: 20532540]

[26]. Jellinger K, Jirasek A. Neuroaxonal dystrophy in man: Character and natural history. Acta Neuropathol. 1971; 5(suppl):3–16. [PubMed: 5562691]

[27]. Kayed R, Sokolov Y, Edmonds B, McIntire TM, Milton SC, Hall JE, Glabe CG. Permeabilization of lipid bilayers is a common conformation-dependent activity of soluble amyloid oligomers in protein misfolding diseases. J Biol Chem. 2004; 279:46363–46366. [PubMed: 15385542]

[28]. Kitamoto T, Muramoto T, Hilbich C, Beyreuther K, Tateishi J. N-terminal sequence of prion protein is also integrated into kuru plaques in pateints with Gerstmann-Straussler-syndrome. Brain Res. 1991; 545:319–321. [PubMed: 1677605]

[29]. Lasmezas CI, Deslys JP, Robain O, Jaegly A, Beringue V, Peyrin JM, Hauw J, Rossier J, Dormont D. Transmission of the BSE agent to mice in the the absence of detectable abnormal prion protein. Science. 1997; 275:402–405. [PubMed: 8994041]

[30]. Liberski, PP.; Yanagihara, R.; Budka, H.; Gajdusek, DC. Light and Electron microscopic neuropathology of slow virus disorders. CRC Press; Boca Raton: 1993. Neuroaxonal dystrophy in unconventional slow virus disease; p. 269-294.

[31]. Liberski PP, Yanagihara R, Gibbs CJJ, Gajdusek DC. Scrapie as a Model for Neuroaxonal Dystrophy: Ultrastructural Studies. Exp Neurol. 1989; 106:133–141. [PubMed: 2806455]

[32]. Manson J, McBride P, Hope J. Expression of the PrP Gene in the Brain of *Sinc* Congenic Mice and its Relationship to the Development of Scrapie. Neurodegeneration. 1992; 1:45–52.

[33]. Manson JC, Jamieson E, Baybutt H, Tuzi NL, Barron R, McConnell I, Somerville R, Ironside J, Will R, Sy MS, Melton DW, Hope J, Bostock C. A single amino acid alteration (101L) introduced into murine PrP dramatically alters incubation time of transmissible spongiform encephalopathy. Embo J. 1999; 18:6855–6864. [PubMed: 10581259]

[34]. McGovern G, Brown KL, Bruce ME, Jeffrey M. Murine scrapie infection causes an abnormal germinal centre reaction in the spleen. J Comp Pathol. 2004; 130:181–194. [PubMed: 15003476]

[35]. Parchi P, Chen SG, Brown P, Zou WQ, Capellari S, Budka H, Hainfellner J, Reyes PF, Golden GT, Hauw JJ, Gajdusek DC, Gambetti P. Different patterns of truncated prion protein fragments correlate with distinct phenotypes in P102L Gerstmann-Straussler-Scheinker disease. Proc Natl Acad Sci. 1998; 95:8322–8327. [PubMed: 9653185]

[36]. Piccardo P, Dlouhy SR, Lievens PMJ, Young K, Thomas DP, Nochlin D, Dickson DW, Vinters HV, Zimmerman TR, Mackenzie IRA, Kish SJ, Ang LC, DeCarli C, Pocchiari M, Brown P, Gibbs CJ, Gajdusek DC, Bugiani O, Ironside J, Tagliavini F, Ghetti B. Phenotypic variability of Gerstmann-Straussler-Scheinker disease is associated with prion protein heterogeneity. J Neuropathol Exp Neurol. 1998; 57:979–988. [PubMed: 9786248]

[37]. Piccardo P, Ghetti B, Dickson DW, Vinters HV, Giaccone G, Bugiani O, Tagliavini F, Young K, Dlouhy SR, Seiler C, Jones CK, Lazzarini A, Golbe LI, Zimmerman TR, Perlman SL, Mclachlan DC, Stgeorgehyslop PH, Lennox A. Gerstmann-Straussler-Scheinker disease (PRNP P102L):

Amyloid deposits are best recognized by antibodies directed to epitopes in PrP region 90-165. J Neuropathol Exp Neurol. 1995; 54:790–801. [PubMed: 7595652]

[38]. Piccardo P, Manson JC, King D, Ghetti B, Barron RM. Accumulation of prion protein in the brain that is not associated with transmissible disease. Proc Natl Acad Sci U S A. 2007; 104:4712–4717. [PubMed: 17360589]

[39]. Prusiner, SB.; Peters, P.; Kaneko, K.; Taraboulos, A.; Lingappa, V.; Cohen, FE.; DeArmond, SJ. Cell biology of prions. In: Prusiner, SB., editor. Prion Biology and Diseases. Cold Spring Harbor Laboratory Press; 1999. p. 349-391.10 Skyline Drive/Plainview/NY 11803-2500/USA

[40]. Somerville RA. TSE agent strains and PrP: reconciling structure and function. Trends Biochem Sci. 2002; 27:606–612. [PubMed: 12468229]

[41]. Tagliavini F, Lievens PMJ, Tranchant C, Warter JM, Mohr M, Giaccone G, Perini F, Rossi G, Salmona M, Piccardo P, Ghetti B, Beavis RC, Bugiani O, Frangione B, Prelli F. A 7-kDa prion protein (PrP) fragment, an integral component of the PrP region required for infectivity, is the major amyloid protein in Gerstmann-Straussler-Scheinker disease A117V. J Biol Chem. 2001; 276:6009–6015. [PubMed: 11087738]

[42]. Tateishi J, Kitamoto T, Hoque MZ, Furukawa H. Experimental transmission of Creutzfeldt-Jakob disease and related diseases to rodents. Neurol. 1996; 46:532–537.

[43]. Tremblay P, Ball HL, Kaneko K, Groth D, Hegde RS, Cohen FE, DeArmond SJ, Prusiner SB, Safar JG. Mutant PrPSc conformers induced by a synthetic peptide and several prion strains. J Virol. 2004; 78:2088–2099. [PubMed: 14747574]

[44]. Wadsworth JD, Joiner S, Linehan JM, Cooper S, Powell C, Mallinson G, Buckell J, Gowland I, Asante EA, Budka H, Brandner S, Collinge J. Phenotypic heterogeneity in inherited prion disease (P102L) is associated with differential propagation of protease-resistant wild-type and mutant prion protein. Brain. 2006; 129:1557–1569. [PubMed: 16597650]

[45]. Wisniewski HM, Vorbrodt AW, Wegiel J, Morys J, Lossinsky AS. Ultrastructure of the cells forming amyloid fibres in Alzheimer's disease and scrapie. Am J Med Gen. 1990; 7:287–297.

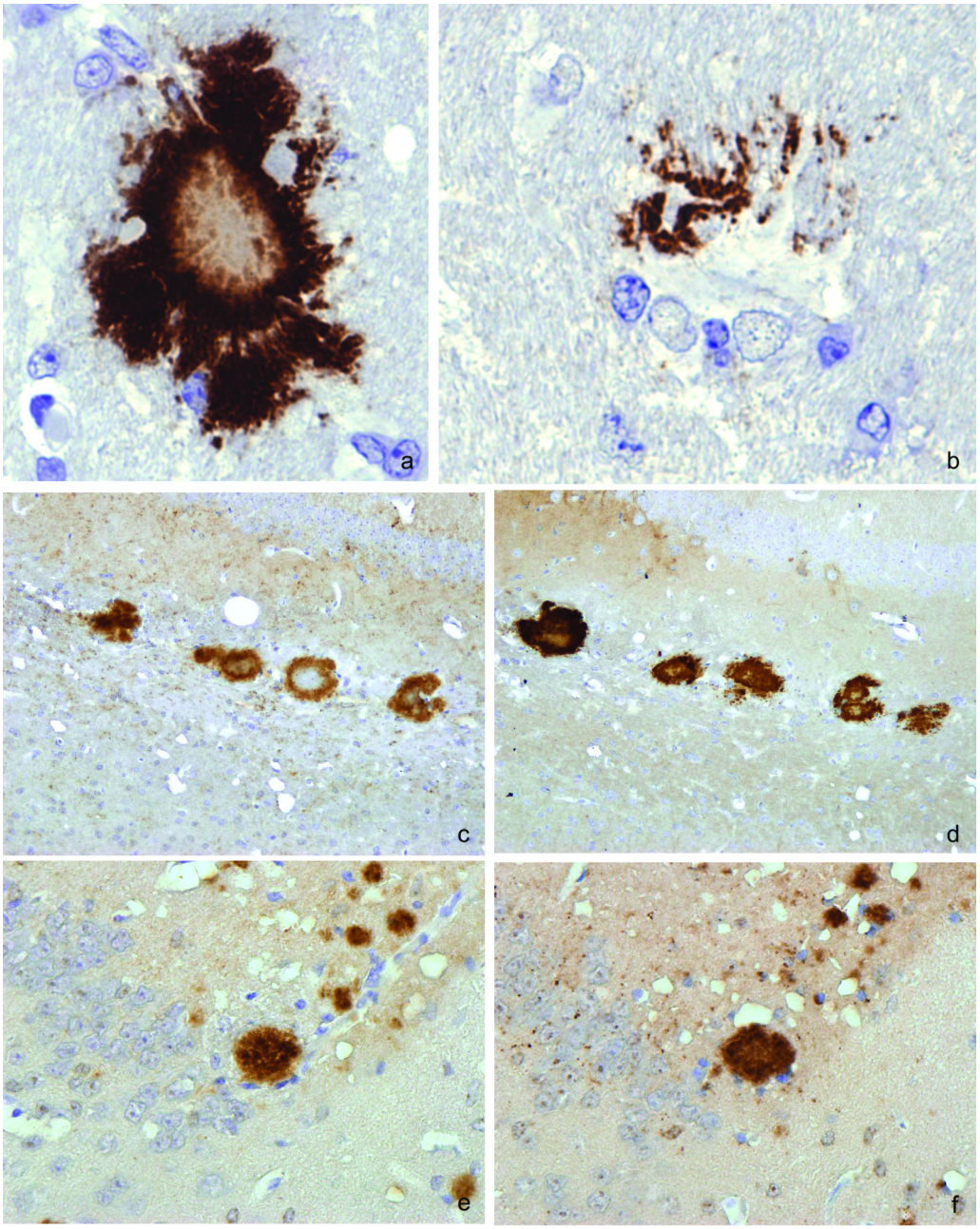

Figure 1.

Plaques in the corpus callosum and adjacent hippocampus of 101LL-8a mice and VM mice with 87V scrapie.

a Mature plaques with an irregular contour and showing central unstained core. Plastic embedded 1 μm thick section labelled with Saf 84 Bar = 16μm

b PrP^d labelling partly surrounding a reactive astrocyte within the corpus callosum. No amyloid was visible in a serial 1μm thick section stained with toluidine blue. Plastic embedded 1 μm thick section labelled with Saf 84 Bar=14 μm

c,d Semi-serial sections of a 101LL-8a mouse showing strong labelling of the periphery of amyloid plaques with R20 (c) and R24 (d) recognising C and N terminal sequences of the PrP protein respectively. Bar=64 μm

e,f; There is no such separate labelling of periphery and core plaques in 87V scrapie with R20 (e) and R24 (f) Bar=32 μm

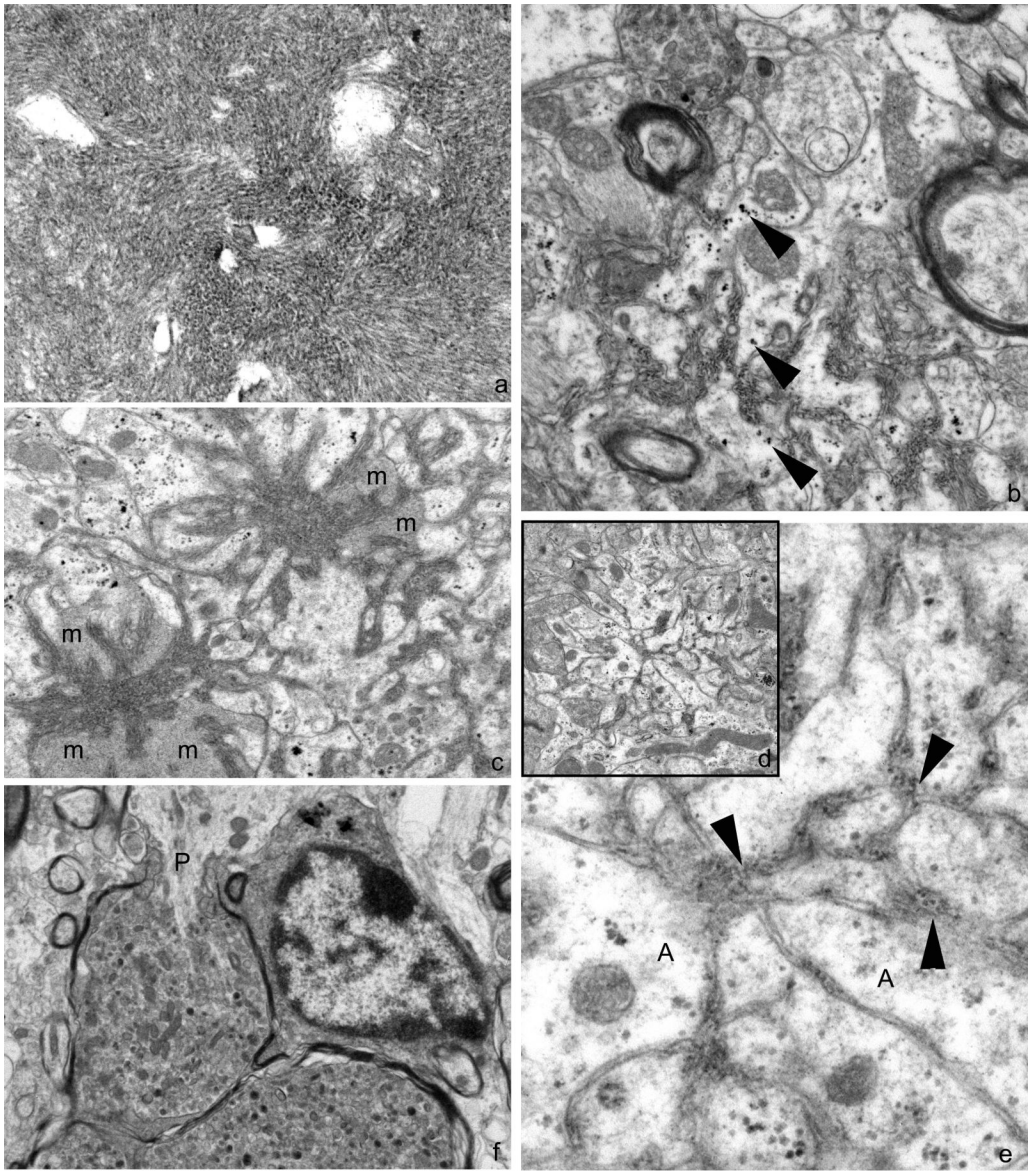

Figure 2.

Electron microscopy of plaques of 101LL-8a mice.

a) the centre of a large plaque showing dense uniform amyloid fibrils arranged in interweaving bundles that virtually exclude all other cellular elements. Bar=225nm

b) The periphery of a large plaque showing infiltration of groups of amyloid fibrils between neuritic and glial processes. Many of the processes belong to astrocytes, identified by the presence of glycogen granules (arrow heads) and the paucity of other sub-cellular organelles. Bar=470nm

c) Two sub-units of a multicentric plaque that was mainly located in grey matter of the Stratum Oriens and which consisted of more than 5 sub-units. Each sub-unit is of similar dimensions, and is surrounded by microglial processes (m). Bar=430nm

d) A small sub-unit of a multicentric plaque. This plaque consists of only a few amyloid fibres within the extracellular space. These fibres are already isolated from neural elements within the adjacent gray matter by astrocytic processes, characterised by their glycogen granules and the paucity of other organelles. Bar =1000nm

e) Detail of D showing the sparse number of amyloid fibres in tangential and transverse section (arrowheads). A, Astrocytic processes. Bar=165nm
f) Dystrophic neurites within myelinated processes adjacent to a large plaque. One dystrophic neurite occupies one side of a paranode (p) while the opposite side appears unaffected. Bar=920nm

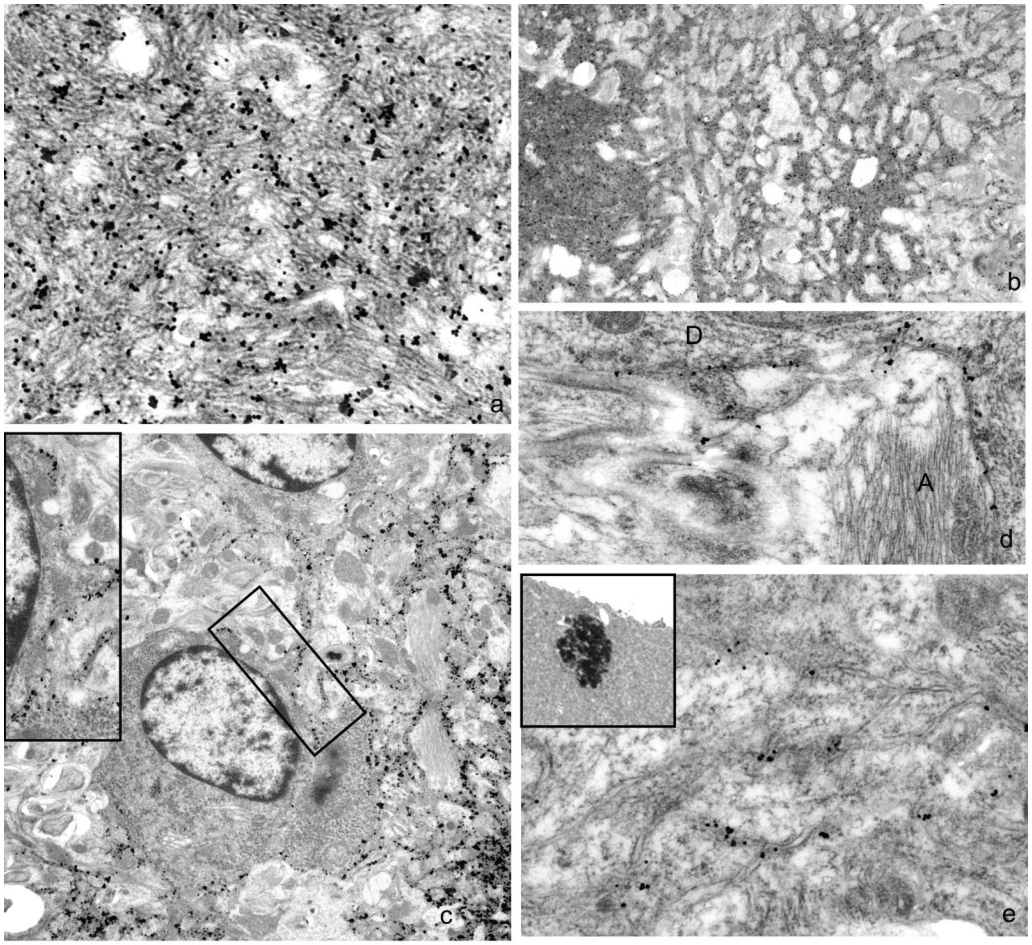

Figure 3.

Immunogold labelling for PrP^d in 101LL-8a mice.

a) Despite the paucity of labelling of plaque cores by light microscopy, the core of a mature plaque shows good immunogold labelling for PrP^d. Bar=138nm.

b) The periphery of a large plaque with one of several smaller adjacent satellite plaques is shown. Both parent and satellite plaques are labelled for PrP^d. Bar=1600nm

c) PrP^d labelling is present around an oligodendrocyte located at the extreme periphery of a large plaque, the edge of which is seen at the bottom right. (Box indicates area shown in inset (inset: showing the localisation of PrP^d on the membranes of the oligodendrocyte). Bar=1600nm

d) Extreme periphery of a plaque. No amyloid fibrils are visible but PrP^d labels the plasma-membrane membranes of several processes including that of a dendrite (D) and an astrocyte (A). Bar=336nm

e) A plaque identified by immunolabelling in the plastic section (inset) shows no morphological change by uranyl acetate/lead citrate staining but in the corresponding location, there is membrane PrP^d labelling on several neuritic processes or in the associated extracellular space. Bar=290nm

Immunogold for PrP^d using 1A8 antibody.

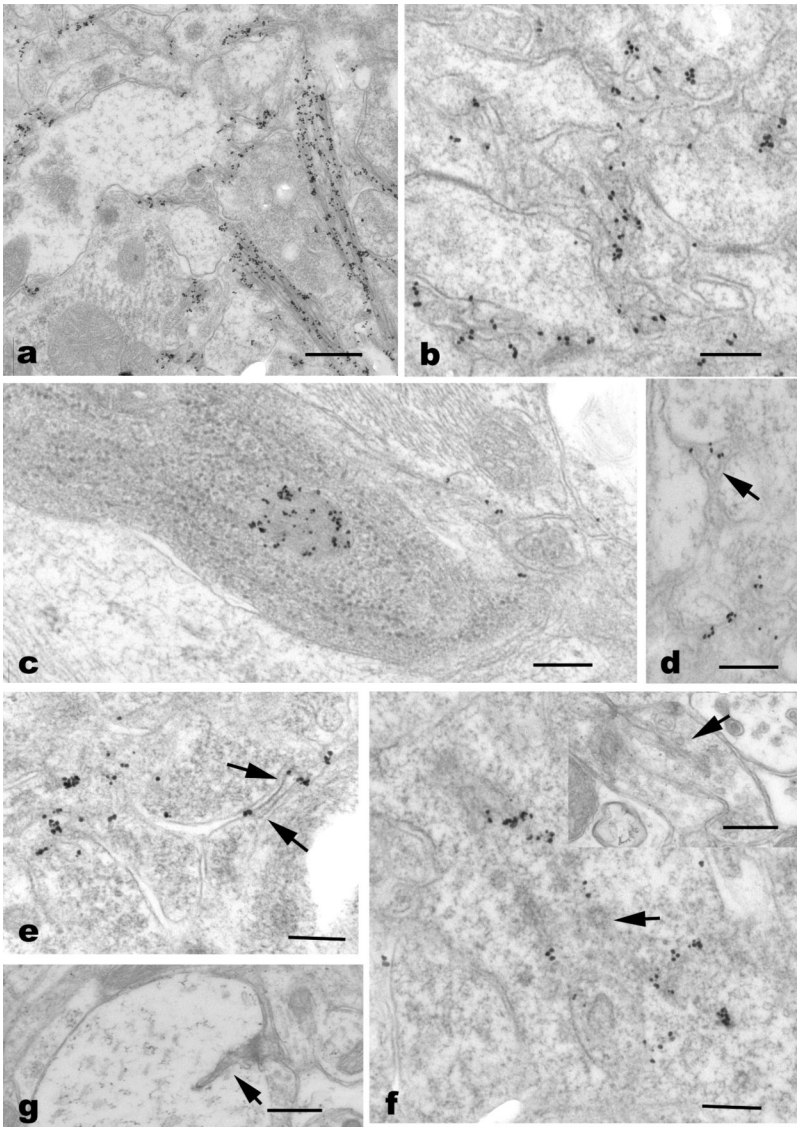

Figure 4.

Features of plaques in 87V infected VM mice.

a) PrP^d labelling of small numbers of amyloid fibrils in longitudinal, transverse and tangential section in the extracellular space at the periphery of a large unicentric plaque. Bar = 275nm

b) PrP^d labelling on the plasma lemma of neurites and glial processes at the extreme periphery of a unicentric plaque. All processes have abnormal irregular contours. No fibrils are evident. Bar =160nm

c) PrP^d labelling of a lysosome within a microglial cell body near the edge of a plaque shown only by sparse PrP^d labelling on cell membranes of adjacent processes Bar=200nm

d and e) PrP^d labelling of small membrane protrusions or microfolds in transverse (arrow in d) and longitudinal (arrows in e) section. d and e Bars =200nm.

f) PrP^d labelling associated with a coated spiral membrane inclusion in an axon terminal. The continuity of the inclusion with the axonal plasma-membrane is not in the plane of section. The abnormal coated vesicles that are associated with these invaginations (arrow) is also clearly evident. The insert shows a further axon terminal membrane invagination. In

this non-immunolabelled section the continuity with the external plasma-membare and the spiral nature of the membrane invagination is evident as are intact synaptic vesicles confirming the process as an axon terminal. Bar=180nm (Bar in insert = 250nm)
g) Part of an abnormal dendrite lacking organelles with an uncoated spiral plasma-membrane invagination. The section is not immunolabelled. Bar = 280nm